INTERACTIVE CONTROL ENGINEERING
Principles and Applications

Volume 20 Motion Control, Robotics, and Autonomous Systems

CHAPTER 4

Lift-Plus-Cruise VTOL Simulator for Control Allocation and Measured Transition Gates

Pages 79–103

Edited by John D. Hedengren

How to cite this chapter. "Lift-Plus-Cruise VTOL Simulator for Control Allocation and Measured Transition Gates," in *Motion Control, Robotics, and Autonomous Systems*, John D. Hedengren, Ed., vol. 20 of *Interactive Control Engineering: Principles and Applications*. Advanced Process Solutions, LLC, 2026, ch. 4, pp. 79–103.

The page numbers in this file are those of the printed volume.

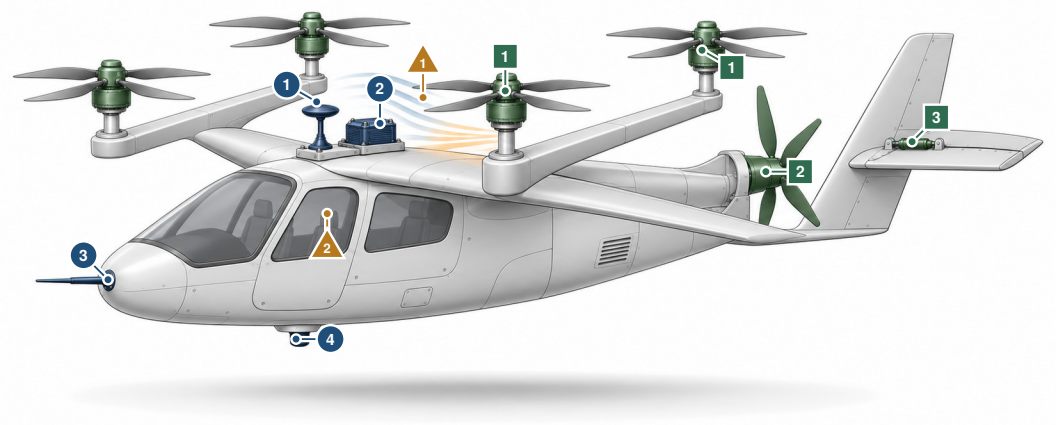
The app for this chapter
https://apmonitor.com/apps/vtol-transition/

The volume online: contents, other chapters and citation records
https://apmonitor.com/apps/books/v20-motion-robotics/#vtol-transition

Copyright © 2026 Advanced Process Solutions, LLC. All rights reserved. Produced by Advanced Process Solutions, LLC.

CHAPTER 4

Lift-Plus-Cruise VTOL Simulator for Control Allocation and Measured Transition Gates



The controller moves 1 front and rear lift rotors 2 pusher propeller 3 elevator on the tail

The controller reads 1 satellite receiver (position and speed) 2 inertial unit (pitch) 3 pitot probe (airspeed) 4 radar altimeter (height)

What disturbs it 1 gust from behind 2 payload in the cabin

Notice the lift rotors, the wing and the pusher on one airframe: in transition the wing takes the weight from the rotors, and the measured airspeed tells when it can carry all of it. Illustration, not to scale.

IN PLAIN TERMS **Handing the Weight From Rotors to a Wing**

The main idea. This electric aircraft lifts off on spinning rotors like a large drone, then flies on its wing like a small plane. The rotors need about three times the power of wing flight, so they stop once the wing can hold the aircraft up.

The challenge. A wing holds the aircraft up only while air flows fast over it, and a gust from behind steals some of that flow. A stop set by the clock can then come too early, while one that waits for the measured airspeed stays safe.

Why it matters. Stopping the rotors too soon makes a loaded aircraft sink toward the trees below it.

THREE WAYS TO READ THIS CHAPTER

Explore	9 min	the first page, the fact on concept vehicles in the Introduction, the history of the first tilt rotor conversion (Section 4.2), the try-it segment, the history of the treetop conversion and the fact on the graded mission (Section 4.6), and the key points
Study	50 min	the whole chapter with its three pause points and the twelve exercises at its end
Practice	15 min	the first page, the measured cases (Section 4.6), Technology in Practice (Section 4.7), Limitations (Section 4.8) and the open challenge

The control question A lift-plus-cruise aircraft hovers on lift rotors that draw about three times the power of wingborne cruise, so every flight hands the weight from the rotors to the wing and back. When may the rotors stop, and should a clock or a measurement decide?

Learning objectives

- Compute the stall, stop and restart speeds of the wing from the weight, and the lift capacity at a rotor stop.
- Explain how a wing-first allocation shares one vertical demand between the wing and two lift-rotor groups.
- Compare a transition timed on the clock with one gated on measurements in a gust and with a heavier load.
- Describe how a lift-derived airspeed exposes a biased pitot.
- Check whether a vertical landing is still feasible after a motor fails.

Prerequisites Sections 1.4.7 (allocation), 1.4.3 (disturbance observer), 1.4.4 (jerk-limited references), 1.4.9 (hysteresis) and 1.6.2 (velocity-form PID). Chapter 3 flies a multirotor on a load sheet.

The app https://apmonitor.com/apps/vtol-transition/

See also Volume 4, Chapter 12 and Volume 4, Chapter 13 for one demand shared among actuators with hard limits. Volume 8, Chapter 11 for a switch on the clock against one on a measured breakthrough, and Volume 8, Chapter 7 for a handover between controllers without a bump.

4.1 Introduction

Many plants have more than one way to produce the effort a loop asks for, and the ways differ in cost, in range and in how their effectiveness changes with the operating point. Volume 4, Chapter 12 shares one push among tires, fans and thrusters at three prices. A ship holding station has thrusters that work at any speed and rudders that work only when it moves, and Chapter 6 weights each thruster of such a vessel by its rating. An aircraft combines control surfaces whose authority grows with dynamic pressure with engines whose thrust does not, and control allocation shares one demand among such effectors in aircraft, marine vessels, road vehicles and spacecraft alike [1]. A process plant has the same shape when a cheap utility carries a load up to its limit and an expensive one supplies the rest. When an effector is switched off rather than merely limited, the plant also becomes a switched system, and the rule that selects the mode belongs to the design, since switching among modes that are each stable can still destabilize the whole [2]. The same choice between a switch on the clock and a switch on a measurement decides when the lead column of Volume 8, Chapter 11 comes off.

An electric lift-plus-cruise aircraft is an extreme case of both. Its lift rotors carry the weight at any airspeed, including none, while its wing carries the weight only above a certain airspeed and below the angle of attack at which it stalls, and the rotors cost several times the power of the wing. NASA's concept vehicles for urban air mobility include a lift-plus-cruise configuration [3], and a physics-based analysis of electric vertical takeoff and landing aircraft found them efficient when cruising but costly in takeoff and climb [4]. In the simulator of this chapter the rotors carry the 19.62 kN weight of a 2000 kg aircraft on 431 kW in hover, while wingborne cruise at 60 m/s with the rotors stopped takes 139 kW. Between the two, the transition hands the weight to the wing, and a supervisor decides when the unloaded rotors may stop and when they must start again. Control design for winged electric aircraft has mostly addressed hover or cruise, although transition needs the rotorcraft and the airplane effectors together [5].

The misconception at stake is that a transition is an event on a schedule, timed once for a nominal aircraft and then replayed. A schedule on the clock and a gate on the measurements make nearly the same decision at the weight and in the air the schedule was tuned for, and in calm air with 250 kg of payload they stop the rotors 42.0 and 43.0 s into the transition, at 49.8 and 51.5 m/s. They part when the load and the air change. With 470 kg on board and a gust from behind at the handover, the schedule stops the rotors at 37.9 m/s, below the 40.4 m/s stall speed of the heavier aircraft, where

no angle of attack can hold the weight, and the aircraft sinks to 9.3 m above a wood. The measured gates keep the rotors turning through the gust and stop them at 55.7 m/s. A transfer function at one operating point represents neither the airspeed on which the wing's effectiveness depends nor the discrete removal of an actuator. Surveys of control teaching and of process control practice recommend laboratory and simulation work in which the plant's behavior, not algebra, carries the lesson [6, 7].

> ✦ **DID YOU KNOW? Eight Lift Rotors and One Pusher**
>
> A lift-plus-cruise concept vehicle described by NASA in 2018, sized for a payload of 1,200 pounds or up to six passengers, has eight lifting rotors and a single pusher propeller. Aircraft of this type have been designed with as few as 4 and as many as 12 lifting rotors [3]. The aircraft of this chapter has eight, lumped into two groups.

However, the two policies can be told apart only in air they were not designed for, and only on a model that carries the physics separating them, lift that follows the air-relative velocity and ends at a stall, rotors that take time to spin up, an allocation that honors every limit and reports what it cannot meet, and sensors that can be wrong. This chapter sets a transition scheduled on the clock against one gated on measurements in a lift-plus-cruise simulator, and shows from the envelope of the wing why the two part company. Lift-plus-cruise transition control, daisy-chain allocation, hysteresis in switching logic and synthetic airspeed are all established methods, and the chapter uses them as they are. Section 4.2 traces the handover from the lift engines of early VTOL aircraft to electric rotors. Section 4.3 builds an eleven-state planar aircraft with air-relative aerodynamics and an explicit stall, momentum-theory power in edgewise flow and a battery power limit, each stated with its constants. Section 4.4 derives closed-form speeds, from the weight and the wing, that locate every gate of the transition, and the lift capacity at the moment of the stop, which predicts the sink that follows. Section 4.5 describes the loops, the constrained allocator and the supervisor with measured gates, feasibility checks and a pitot cross-check. Section 4.6 flies eight cases and a graded mission that isolate the handover, the envelope, the back-transition, a gust, a heavier load, a sensor fault and a motor failure. Section 4.7 names the airspeed sensor, the lift rotors and the flight computer of a real aircraft, Section 4.8 states what the model leaves out, and Section 4.9 draws the lessons together.

4.2 Transition Flight From Lift Engines to Electric Rotors

An aircraft that takes off vertically and cruises on a wing has to hand its weight from one source of lift to the other, and two answers appeared early. One keeps lift and cruise thrust apart. Lift engines used only for vertical flight were evaluated for tactical VTOL aircraft in 1965 [8], and in 1968 a primary fly-by-wire flight control system was designed and developed for the XV-4B V/STOL research aircraft [9]. The other turns one set of thrusters from lifting to propelling, as the XV-15 tilt rotor research aircraft did in a program reported in 1979 [10]. The electric lift-plus-cruise aircraft returns to the first answer with rotors in place of jets, since its lift rotors are stopped in cruise and a separate pusher propels it.

The physics of the handover is older than either. Glauert's momentum theory of the autogyro related the induced velocity of a rotor to its thrust and to the flow through it in forward flight [11], and the same relation, with a figure of merit for the losses, gives the power of the lift rotors in this model. A fixed wing's lift follows its angle of attack up to the stall and then falls toward the normal force of a flat plate, and flight models of small aircraft join the two regimes with a sigmoid in the angle of attack [12].

The distribution of one demand among redundant, limited effectors became a subject of its own with aircraft control surfaces. Constrained control allocation described the moments that limited surfaces can attain [13], and daisy-chain allocation uses one group of effectors until it saturates and passes the remainder to the next [14]. The allocator of this chapter is a daisy chain in that sense, with

the wing first and the rotors second, and it reaches the wing only through the pitch attitude. The general choices of an allocation at its limits are set out in Section 1.4.7.

Electric aircraft revived the problem at a new scale. NASA's concept vehicles for urban air mobility include a lift-plus-cruise design, generic by intent and different in detail from industry arrangements [3, 15]. Transition control laws for such an aircraft have been designed to meet flying-qualities requirements within realistic motor limits, with variable rotor speed sufficient at low speed where the control surfaces lack authority [5]. An airspeed-dependent blending between hover and fixed-wing controllers has been analyzed for stability near the stall, with different responses in the two directions of transition [16], and an automatic flight and transition system for a lift/cruise VTOL aircraft has been verified in flight [17]. The airspeed on which such schedules rest comes from a pitot tube, and a synthetic air data system has been used to detect pitot tube failure on a variable-skew quad plane [18]. The cross-check of this chapter is of that kind, an airspeed inferred from the lift the wing is measured to make.

> ⧖ HISTORY **Converting a Tilt Rotor in Flight (1979)**
>
> A tilt rotor research aircraft flew its first full conversion from helicopter to airplane mode on 24 July 1979. It had taken 15 hours of flight tests over more than three months, widening the envelope in small steps of airspeed and nacelle angle. The wing's control surfaces stayed active in every configuration. As the nacelles tilted toward the airplane position, two mechanical mixing boxes phased the rotor controls out automatically, so the pilot mainly had to hold the attitude while the heavy nacelles moved. The conversion could be flown anywhere in a corridor of airspeeds and nacelle angles, bounded at low airspeed by the stall of the wing [19]. The handover of control followed the nacelle angle, and the wing's stall set how slow it could be flown.

4.3 A Planar Lift-Plus-Cruise Aircraft

The simulated aircraft belongs to the lift-plus-cruise class, 1750 kg empty with 250 kg of payload as shipped, and its flight is confined to the vertical plane through the route. Its eight lift rotors on two booms are lumped into a front and a rear group with one thrust each, a pusher propeller sits at the tail and a wing over the center of mass. Distance x points forward along the route, the altitude z of the landing gear points up and the pitch θ is positive nose up, so the body's forward axis is $(\cos\theta, \sin\theta)$ and its up axis $(-\sin\theta, \cos\theta)$. The values are illustrative and describe no particular aircraft. The geometry, the forces and the instruments are shown in Figure 4.1.

Table 4.1 sorts the signals by role. The eleven integrated states are the distance and the altitude with their rates, the pitch and its rate, the thrusts of the two lift groups and of the pusher, the elevator deflection and the energy left in the battery.

4.3.1 Forces, Moments and Mass

The lift rotors push along the up axis and the pusher along the fuselage, which with the aerodynamic force $\mathbf{F}_a$ gives the translational balance of Equation (4.1).

$$\begin{aligned} m\ddot{x} &= F_{a,x} - T_R \sin\theta + T_p \cos\theta \\ m\ddot{z} &= F_{a,z} + T_R \cos\theta + T_p \sin\theta - mg, \qquad T_R = T_f + T_r \end{aligned} \tag{4.1}$$

The pitch balance of Equation (4.2) takes each group's arm from the center of mass.

$$\begin{aligned} I\ddot{\theta} = \bar{q}S\bar{c}\left[C_m(\alpha) + C_{mq}\frac{\omega\bar{c}}{2V} + C_{m\delta}\delta_e\right] \\ + \ell_f T_f - \ell_r T_r - h_p T_p \end{aligned} \tag{4.2}$$

where $\bar{q} = \rho V^2/2$ is the dynamic pressure of the air-relative speed V, $\omega = \dot{\theta}$ the pitch rate, $\ell_f = \ell - c$ and $\ell_r = \ell + c$, with c the position of the center of mass ahead of the rotors' centroid. The damping term acts only above 0.5 m/s. A level hover in still air needs $\ell_f T_f = \ell_r T_r$, so with $c = -0.15$ m the

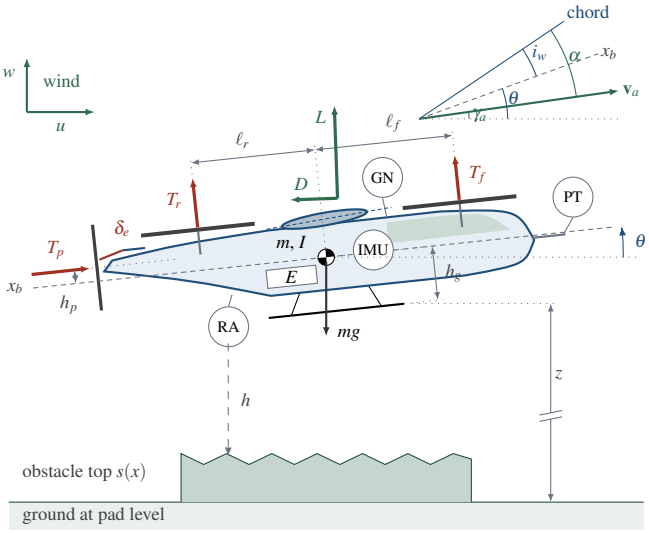


Figure 4.1 The planar lift-plus-cruise aircraft as modeled, drawn with a 6° pitch and not to scale in height. The front and rear lift groups push along the body's up axis with T_f and T_r at arms $\ell_f = \ell - c$ and $\ell_r = \ell + c$ from the center of mass, which sits 0.15 m behind the rotors' centroid ($c = -0.15$ m). The pusher T_p acts along the fuselage h_p above the center of mass, the elevator δ_e at the tail, and the wing at incidence i_w makes lift L normal and drag D parallel to the air-relative velocity $\mathbf{v}_a$. The key defines γ_a, θ, i_w and α with exaggerated angles. GN, IMU, PT and RA are the GNSS receiver $(x_m, z_m, v_{x,m}, v_{z,m})$, the inertial unit (θ_m, ω_m), the pitot (V_p) and the radar altimeter (h_m), E is the battery, h_g the height of the center of mass above the gear, z the gear altitude above the pad level and h the height above the surface $s(x)$ below.

Table 4.1 Variables, With Nominal Values in the Hover of Case 1 and in Wingborne Cruise at 60 m/s

Symbol	Role	Hover, cruise	Range
z	CV, gear altitude	50, 110 m	SP 30–200 m
$\dot{x}$	CV, ground speed	0, 60 m/s	SP 35–75 m/s
x	CV, position trim	0, —	0–7 km
θ	CV, pitch loop	0, 0.08°	−8 to 15°
a_z, a_x	MVs, accelerations	0, 0	±5, ±3 m/s^2
M	MV, pitch moment	0, 0	±60 kN m
T_f	state, front group	9.30 kN, 0	0–16 kN
T_r	state, rear group	10.32 kN, 0	0–16 kN
T_p	state, pusher	0, 1.78 kN	−1.5 to 5.5 kN
δ_e	state, elevator	0, −1.59°	−25 to 20°
$\dot{x}$, $\dot{z}$, ω	states, rates	0	—
E	state, battery energy	120 kWh	0–150 kWh
—	MV of the supervisor	rotors on, off	4 states
m_{pay}	DV, payload	250 kg	0–500 kg
u_0, s_t	DV, wind, turbulence	0, 1	±12 m/s, 0–2
b_p	DV, pitot bias	0	±15 m/s
a_r	DV, rear authority	100 %	25–100 %
—	DV, gust, updraft, failure	events	—

rear group carries $\ell_f/(\ell_f + \ell_r) = 52.6\,\%$ of the weight, 10.32 kN against 9.30 kN at 2000 kg. Payload adds mass and inertia, $m = m_e + m_{pay}$ and $I = I_0 + m_{pay} r_{pay}^2$, which gives 2000 kg and 5250 kg m^2 as shipped, and it changes only on a pad, before a run starts or at a Reset, which restarts the case with it.

4.3.2 Air-Relative Aerodynamics and the Stall

The wing's forces follow the velocity relative to the air, $\mathbf{v}_a = (\dot{x}-u, \dot{z}-w)$ with u and w the wind, as shown in Equation (4.3).

$$\begin{aligned} V &= |\mathbf{v}_a|, \quad \gamma_a = \operatorname{atan2}(v_{a,z}, v_{a,x}), \quad \alpha = \theta + i_w - \gamma_a \\ F_{a,x} &= -\frac{D v_{a,x} + L v_{a,z}}{V}, \quad F_{a,z} = \frac{L v_{a,x} - D v_{a,z}}{V} \\ L &= \bar{q} S C_L(\alpha), \quad D = \bar{q} S C_D(\alpha) \end{aligned} \tag{4.3}$$

Lift is normal to $\mathbf{v}_a$ and drag lies along it, so both vanish at zero airspeed, and a gust from behind removes lift at constant ground speed. The coefficients of Equation (4.4) are linear up to the stall and blend into a flat plate past it [12].

$$\begin{aligned} \sigma &= \left[1 + \mathrm{e}^{-M_s(|\alpha| - \alpha_s - \Delta_s)}\right]^{-1}, \qquad C_{L,lin} = C_{L0} + a\alpha \\ C_L &= (1-\sigma) C_{L,lin} + \sigma C_N \sin\alpha \cos\alpha \\ C_D &= (1-\sigma)\left(C_{D0} + k C_{L,lin}^2\right) + \sigma\left(C_{D0} + C_N \sin^2\alpha\right) \\ C_m &= (1-\sigma)\left(C_{m0} + C_{m\alpha}\alpha\right) - \tfrac{1}{2}\sigma \sin\alpha \end{aligned} \tag{4.4}$$

where $M_s = 80\,\mathrm{rad}^{-1}$ sets the sharpness and the offset $\Delta_s = 1.92^\circ$ places the lift peak at the stall angle $\alpha_s = 14^\circ$. There C_L peaks at 1.359, and by 18° it has fallen to 0.621 while C_D has risen from 0.137 to 0.215. The stopped rotors' drag is folded into C_{D0}, and the rotors and the wing do not interfere.

4.3.3 Rotor, Pusher and Battery Power

Each spinning lift group draws the power of Equation (4.5), in which the induced velocity in edgewise flow follows Glauert's momentum theory [11].

$$\begin{aligned} P_i &= \frac{T_i\left[v_i + \max(0, V_c)\right]}{FM} + P_0, \qquad v_h^2 = \frac{T_i}{2\rho A} \\ v_i &= \left[\frac{2 v_h^4}{\sqrt{V_e^4 + 4 v_h^4} + V_e^2}\right]^{1/2} \end{aligned} \tag{4.5}$$

for $i \in \{f, r\}$, where V_e and V_c are the components of $\mathbf{v}_a$ along the fuselage and the up axis, A the disk area of one group, FM the figure of merit on the induced part and P_0 the profile power of a spinning group. A stopped group draws nothing, and a descent earns no credit. In hover $v_i = v_h$, and the two groups draw 420.5 kW at 2000 kg, against an ideal induced power of 277.9 kW, an effective figure of merit of 0.661. The pusher and the battery follow Equation (4.6).

$$\begin{aligned} P_p &= \frac{|T_p|\left(V_f + v_{ip}\right)}{\eta_p}, \qquad v_{ip} = -\frac{V_f}{2} + \sqrt{\frac{V_f^2}{4} + \frac{|T_p|}{2\rho A_p}} \\ \dot{E} &= -\left(P_f + P_r + P_p + P_{av}\right), \qquad P \le P_{max} f(E/E_{cap}) \\ f(s) &= \min\left(1,\ p_f + (1-p_f)\, s/s_k\right) \end{aligned} \tag{4.6}$$

where $V_f = \max(0, V_e)$ for forward thrust and zero in reverse, P_{av} is the avionics and cabin power, and the limit falls linearly below the knee s_k to p_f of P_{max} at empty. The two groups, the pusher and the elevator each lag their commands with a first-order time constant, $\tau \dot{T}_i = T_{i,cmd} - T_i$, and the commands are rate limited before they are sent. A stopped group's thrust below 5 N is zeroed after each step.

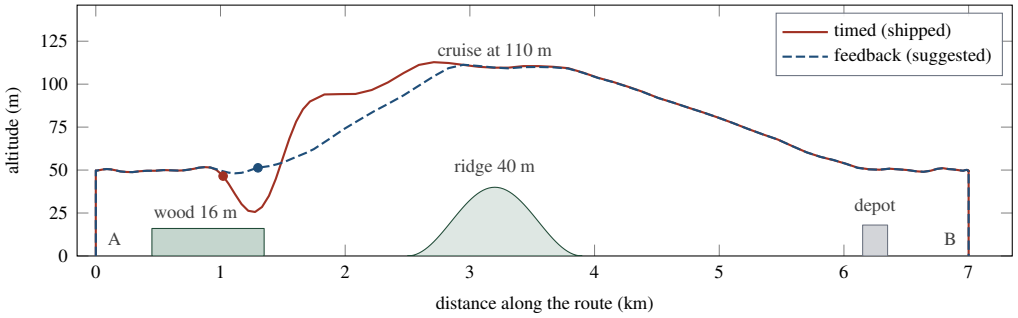


Figure 4.2 The route and the two flights of the challenge, gear altitude against distance, with the timed transition as shipped (solid) and with the suggested feedback transition (dashed). The dot on each line marks its rotor stop command. The timed flight sinks to 25.4 m over the wood, 9.3 m above the trees, and then climbs through its reference, while the feedback flight never falls more than 1.9 m below its reference. Both flights brake to rest over pad B and descend onto it. The vertical scale is exaggerated.

4.3.4 Wind, Route and Contact

The wind of Equation (4.7) is a steady component along the route, one-minus-cosine gusts and first-order colored turbulence, sampled at each control step and held until the next, and the same over the whole airframe.

$$\begin{aligned} u &= u_0 + \textstyle\sum_j \Delta u_j \, g_j(t) + 0.8 \, s_t n_u \\ w &= \textstyle\sum_j \Delta w_j \, g_j(t) + 0.5 \, s_t n_w \\ g_j &= \tfrac{1}{2}\left[1 - \cos\!\big(2\pi(t - t_j)/D_j\big)\right], \quad t_j \le t \le t_j + D_j \end{aligned} \tag{4.7}$$

where n_u and n_w have unit standard deviation and correlation times of 2 and 1 s, the scale s_t is 1 in every case, and u is positive from behind. The gust event adds $\Delta u = 8\,\mathrm{m/s}$ over $D = 8\,\mathrm{s}$, and cases 5 and 9 use 10 m/s with $\Delta w = -1\,\mathrm{m/s}$ over 10 s.

The route runs 7 km from pad A to pad B over a wood of 16 m trees from 450 to 1350 m, a ridge that rises to 40 m as a raised cosine from 2500 to 3900 m, and an 18 m depot from 6150 to 6350 m, as shown in Figure 4.2, and a diversion airfield lies 8 km beyond pad B. A touchdown occurs when the gear reaches the surface while descending, except in the 0.5 s after a liftoff. Within 7.5 m of a pad center it is a landing unless the sink exceeds 3.0 m/s or the pitch 10°, and anywhere else it is a crash, as is any contact of the nose, the tail or a boom tip with the ground or an obstacle. Liftoff requires the rotors and the wing to lift more than $1.001\,mg$.

4.3.5 Parameters, Numerics and Initial States

Table 4.2 gives the parameters. The fourth-order Runge-Kutta method integrates the states on a 2 ms step, the control laws execute every 10 ms, and the log records 20 samples per second, on the engine of Section 1.6.1. Halving the step moves the touchdown of the suggested challenge by 0.012 mm/s and 0.047 mm and the energy drawn up to 238.10 s by 0.014 mWh, and its rotor stop stays on the same control step. In the shipped challenge the timed stop comes one control step later at the half step, at 69.12 s, because the summed clock reaches 42 s after the start of the transition a rounding error later, and the two runs' airspeeds agree to 0.01 mm/s at the same instant. A scenario starts on a pad with the rotors stopped, in a hover trimmed for its load, or wingborne at its speed with the rotors stopped and the pitch, pusher and elevator trimmed.

Table 4.2 Aircraft Parameters. Values Not Marked Hidden Can Be Changed in the Model Dialog Within the Range Given

Symbol	Meaning	Value	Range
m_e	operating empty mass	1750 kg	1400–2100
I_0	pitch inertia, empty	5000 kg m^2	3000–8000
r_{pay}	payload radius of gyration	1.0 m	hidden
ℓ, c	arm, c.m. ahead of centroid	2.9, −0.15 m	2–4, ±0.5
h_p, h_g	pusher line, gear	0.3, 1.2 m	−0.5–1, hidden
T_{max}, T_{idle}	group rating, idle	16 kN, 300 N	10–22, 0–1000
τ_R, —	group lag, rate limit	0.15 s, 25 kN/s	0.05–0.5, 5–60
t_{spin}, P_0	spin-up, profile power	2.0 s, 25 kW	0.5–5, 0–60
A, FM	disk per group, merit	20 m^2, 0.75	10–40, 0.5–0.9
$T_{p,max}$, $T_{p,min}$	pusher limits	5.5, −1.5 kN	3–9, −3–0
τ_p, —	pusher lag, rate limit	0.3 s, 10 kN/s	0.05–1, 2–30
A_p, η_p	pusher disk, efficiency	3.1 m^2, 0.85	hidden, 0.6–0.95
S, $\bar{c}$	wing area, chord	16 m^2, 1.42 m	10–25, 0.8–2.5
i_w, α_s	incidence, stall angle	4°, 14°	0–8, 10–18
C_{L0}, a	lift at zero, slope	0.2, 5.0 rad^{-1}	0–0.5, 3.5–6.3
M_s, C_N	sharpness, flat plate	80 rad^{-1}, 1.9	hidden
C_{D0}	zero-lift drag	0.035	0.02–0.08
k	induced-drag factor	0.05	0.03–0.08
C_{m0}, $C_{m\alpha}$	moment, stiffness	0.03, −0.7 rad^{-1}	±0.1, −2–0
C_{mq}	pitch damping	−10	−30–0
$C_{m\delta}$	elevator effectiveness	−1.1 rad^{-1}	−2 to −0.3
δ_e	elevator travel	−25, 20°	−35 to −10, 10–30
τ_e, —	elevator lag, rate	0.05 s, 60 °/s	0.02–0.2, 20–120
ρ, g	density, gravity	1.225, 9.81	1.0–1.3, hidden
E_{cap}	usable battery energy	150 kWh	60–250
P_{max}	rated battery power	700 kW	400–1000
s_k, p_f	sag knee, power at empty	30, 60 %	10–50, 30–100
P_{av}	avionics and cabin	5 kW	0–20
—	gear sink, pitch limits	3.0 m/s, 10°	1–5, 4–20
σ_x, σ_z	GNSS position, altitude	0.3, 0.15 m	0–2, 0–1
σ_v, σ_q	GNSS velocity, pitot	0.05 m/s, 4 Pa	0–0.5, 0–30
σ_θ, σ_ω	attitude, gyro	0.1°, 0.3 °/s	0–1, 0–3

4.3.6 Assumptions

Flight is planar and longitudinal, with no roll, yaw, sideslip or turns, so a go-around on the wing continues ahead to the airfield beyond pad B instead of circling back.

Each group of four rotors becomes a single thrust, lagged, rate limited and given a 2 s spin-up. Inflow dynamics, flapping and the in-plane H-force of the rotors are absent, and so are the rotors' downwash on the wing and the wing's upwash through the rear rotors, which in a real aircraft change both the lift and the rotor power during the transition.

The aerodynamics are quasi-steady, with no dynamic stall or lift lag. A six-degree-of-freedom analysis of lift-plus-cruise transition locates a near-stall region where the short-period damping falls [16], and the angle-of-attack margin the scorecard reports is not a measure of that damping.

Rotor power is momentum theory corrected by one fixed figure of merit and a profile power, without a vortex-ring state. The battery holds energy and limits power, and it has no voltage, temperature or aging dynamics.

The wind is uniform over the airframe, with no shear and no ground effect, and the sensors carry colored noise without latency or dropouts. The controller's aerodynamic model equals the plant's, so its errors come only from what it cannot measure, the vertical gust, the turbulence and a biased pitot. The margins and limits, a 10 % lift-group margin, 3° of angle-of-attack protection, 25 m of clearance and a 20 % energy reserve, are teaching values, not certification requirements.

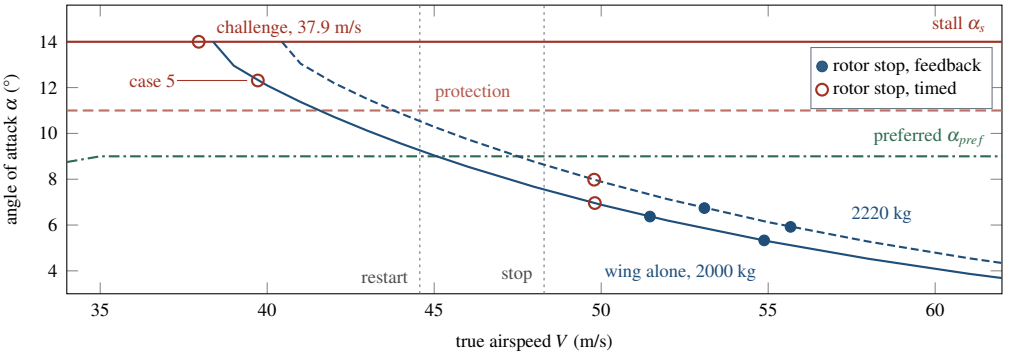


Figure 4.3 The envelope of the handover. The solid and dashed curves give the angle of attack at which the wing alone carries 2000 and 2220 kg in level flight, from the model's own C_L up to the lift peak, and end at the stall speeds of 38.4 and 40.4 m/s. The stall angle is the solid horizontal line, the protection the dashed one and the preferred angle the dash-dotted one. The markers, filled for the feedback transition and open for the timed one, place the true airspeed of each rotor stop command on the curve of its mass. The timed stops of cases 2 and 6 leave the wing margin in hand, the one in the gust of case 5 lies above the protection, and the one in the challenge lies below the stall speed, where no angle holds the weight.

Table 4.3 Transition Speeds From the Weight and the Wing Against the Engine, in m/s

Event	Predicted	Measured
wing takes half the weight, forward (case 2)	32.7	33.5
rotors take half the weight, back (case 4)	32.7	32.7
rotors under 8 % of the weight (case 2)	43.2	42.7
restart gate V_{off}, 2000 kg (case 3)	44.6	44.3
stop gate V_{on}, 2000 kg (case 2)	48.3	48.2
stop after the 2 s dwell (case 2)	50.7	51.5
stop gate V_{on}, 2220 kg (case 6)	50.9	51.0

4.4 Where the Wing Can Take the Weight

Four speeds follow from the weight and the wing alone, and they locate the gates of a transition. In level flight the wing alone carries mg at the angle where $C_L(\alpha) = 2mg/(\rho S V^2)$, so it can carry the weight at all only above the stall speed V_s, and inside the protection only above V_p. The gates of Section 4.5 add the lift margins μ_{on} and μ_{off}, as shown in Equation (4.8).

$$\begin{aligned} V_s &= \sqrt{\frac{2mg}{\rho S C_{L,max}}}, & V_p &= \sqrt{\frac{2mg}{\rho S C_L(\alpha_s - \Delta\alpha_p)}} \\ V_{on} &= V_p\sqrt{1+\mu_{on}}, & V_{off} &= V_p\sqrt{1+\mu_{off}} \end{aligned} \tag{4.8}$$

With $C_{L,max} = 1.359$, $C_L(11°) = 1.159$, $\mu_{on} = 35\,\%$ and $\mu_{off} = 15\,\%$ they are 38.4, 41.6, 48.3 and 44.6 m/s at 2000 kg, and 40.4, 43.8, 50.9 and 47.0 m/s at 2220 kg. Because $V_p = 1.083V_s$, the stop gate lies at $1.258V_s$ and opens after the airspeed gate at $1.2V_s$, which is therefore a backstop at the default settings. The allocation gives the wing what it lifts at a preferred angle α_{pref}, which rises from the fuselage-level 4° below 15 m/s to 9° at 35 m/s, and the rotors the rest. The wing therefore takes half the weight where $\frac{1}{2}\rho V^2 S C_L(\alpha_{pref}(V)) = mg/2$, and the rotors fall under 8 % where it lifts $0.92mg$. The angle the wing alone needs is plotted against the airspeed in Figure 4.3, and the predictions are compared with the engine in Table 4.3.

Table 4.4 Lift Capacity at the Rotor Stop and the Sink That Follows. Capacity Is What the Wing Lifts at 11° at the Stop Airspeed, as a Share of the Weight, and the Loss Is the Largest Distance Below the Altitude Reference in the Next 15 s

Stop	kg	m/s	Capacity	Loss (m)	Drop (m)
feedback, case 2	2000	51.5	153 %	2.5	1.2
feedback, case 5	2000	54.9	174 %	0.9	0
feedback, case 6	2220	53.1	147 %	2.5	1.0
feedback, challenge	2220	55.7	162 %	1.6	0
timed, case 2	2000	49.8	144 %	2.1	0.5
timed, case 6	2220	49.8	129 %	1.8	0.2
timed, case 5	2000	39.7	91 %	6.7	3.2
timed, challenge	2220	37.9	75 %	31.7	21.1

The gates open where Equation (4.8) says, to within 0.1 m/s, because the supervisor evaluates the same expression on an exact load sheet and a pitot that is accurate in calm air. The rotors stop 2.03 s after the gate opens in case 2, while the reference accelerates at 1.2 m/s^2, so the prediction is $48.3 + 2.4 = 50.7\,\mathrm{m/s}$, and the stop comes at a true airspeed of 51.5 m/s with a ground speed of 50.8 m/s, the difference being a 0.7 m/s turbulent headwind. The restart comes 0.3 m/s below its gate because the restart condition must hold for 0.3 s while the aircraft slows. The half-load points fall at and just above the prediction. On the way out the wing takes half the weight at 33.5 m/s, when its true angle of attack trails the commanded 8.65° by 0.54°, and on the way in the rotors carry half at 32.7 m/s.

The capacity at the moment of the stop predicts what follows, as shown in Table 4.4, where the drop is the altitude lost from the stop to the lowest point. Every stop with a capacity of 129 % or more loses less than 2.6 m against a reference that climbs toward the cruise altitude, and loses at most 1.2 m of real height. At 91 % the aircraft drops 3.2 m, and at 75 % it drops 21.1 m. The feedback gates guarantee at least 135 % by construction when the airspeed is right, and delivered 147 to 174 %. The timed schedule guarantees nothing, because its capacity is set by whatever airspeed the clock happens to meet.

4.5 Loops, Allocation and Supervisor

The controller runs every $\Delta t_c = 10\,\mathrm{ms}$ on sampled, noisy measurements, and the true state, airspeed, angle of attack and wind stay hidden from it. Three loops ask for a vertical acceleration, a longitudinal acceleration and a pitch moment, an allocator shares these demands among the wing, the rotors, the pusher and the elevator, and a supervisor runs the mission and decides whether the rotors may turn, as shown in Figure 4.4.

4.5.1 Sensors and Estimators

GNSS gives x_m and z_m with colored noise of 0.3 and 0.15 m and correlation times of 0.5 s, and the two velocities with 0.05 m/s and 0.1 s. The radar altimeter gives the height above what is below with 0.15 m and 0.2 s, and the inertial unit gives θ_m and ω_m with 0.1° and 0.3 °/s at 0.05 and 0.02 s. The pitot measures the dynamic pressure of the airspeed along the fuselage with 4 Pa of noise and a bias b_p, $V_p = \max\big(0, \sqrt{2\max(0, \bar{q}_m)/\rho} + b_p\big)$, which makes it poor below about 10 m/s. The estimators

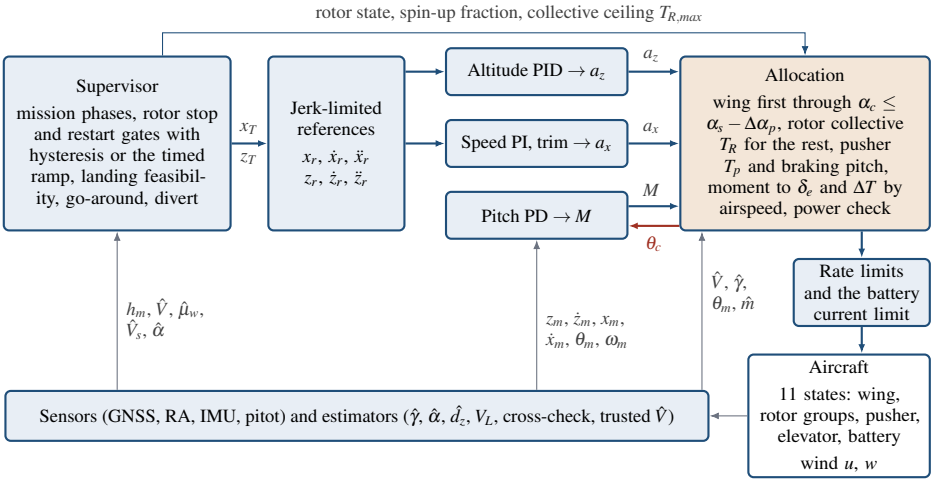


Figure 4.4 The controller as implemented. The allocation writes the pitch loop's setpoint θ_c, which is how it reaches the wing, and the supervisor sets what it may ask of the rotors, through the rotor state and, in the timed transition, a ceiling on the collective. The loops read the measurements, and the allocation and the supervisor also read the estimates, including the trusted airspeed $\hat{V}$.

of Equation (4.9) supply what cannot be measured.

$$\begin{aligned}
\hat{\gamma} &= w_\gamma \arcsin\left(\operatorname{clamp}\left(\frac{v_{z,m}}{\max(\hat{V},10)}, \pm 0.35\right)\right) \\
\hat{\alpha} &= \theta_m + i_w - \hat{\gamma} \\
\dot{\hat{\xi}} &= \hat{F}_z + \hat{d}_z, \qquad \hat{d}_z = K\left(\hat{m} v_{z,m} - \hat{\xi}\right) \\
V_L &= \sqrt{\frac{2\hat{d}_z}{\rho S C_L(\hat{\alpha}) \cos\hat{\gamma}}}
\end{aligned} \tag{4.9}$$

where $w_\gamma = \operatorname{clamp}((\hat{V}-10)/10, 0, 1)$ in m/s, $\hat{F}_z = (\hat{T}_f + \hat{T}_r)\cos\theta_m + \hat{T}_p \sin\theta_m - \hat{m}g$ is built from the controller's own commands through exact models of the actuator lags, $K = 1.5\,\mathrm{s}^{-1}$, and $\hat{m}$ is the load sheet's mass, which is exact. The observer's $\hat{d}_z$ is the vertical aerodynamic force, and V_L, filtered with 0.5 s, is the airspeed at which the wing would make it at $\hat{\alpha}$. The observer is the disturbance observer of Section 1.4.3 applied to the vertical force, and V_L is an analytical redundancy for the pitot. It is formed only above 30 m/s, with $C_L(\hat{\alpha}) > 0.4$ and $\hat{d}_z > 0.3\hat{m}g$. The ratio V_L/V_p is filtered with 1.5 s, a disagreement is a ratio more than 15 % from one, and 2 s of disagreement flags the pitot. The trusted airspeed $\hat{V}$ is the pitot, the lower of the two while they disagree, and V_L once the pitot is flagged, with the pitot's learned error removed below 30 m/s. The estimate $\hat{\alpha}$ cannot see a vertical gust.

4.5.2 The Three Loops

Every loop runs the shared velocity-form PID of Section 1.6.2, written in the symbols of this chapter in Equation (4.10).

$$\begin{aligned}
e_k &= \mathrm{SP}_k - \mathrm{PV}_k, \qquad P_k = K_c e_k \\
S_k &= S_{k-1} + (P_k - P_{k-1}), \qquad c_k = b_k + S_k + I_{k-1} \\
u_k &= \operatorname{clamp}(c_k,\ u_{min},\ u_{max}) \\
I_k &= I_{k-1} + \left[\frac{K_c}{\tau_I} e_k + \frac{u_k - c_k}{T_t}\right] \Delta t_c
\end{aligned} \tag{4.10}$$

It is Equations (1.19) to (1.22) with S_k the running sum of the proportional increments, which is never clamped. Anti-windup is back-calculation with $T_t = \tau_I$, applied only in a loop that integrates, and no loop sets a rate limit. The allocation's own limits, the rotor ceiling, the protected angle and the battery, act after these clamps and are not fed back, so while a lamp reports a demand unmet below the clamp the integral keeps integrating the whole error. The derivative option of the shared PID is left at zero. Each derivative term is built instead from a measured rate and carried in the bias b_k of Equation (4.11), so a setpoint change produces no kick.

$$\begin{aligned} b_z &= \ddot{z}_r + K_{c,z}\tau_{D,z}(\dot{z}_r - v_{z,m}), \qquad b_x = \ddot{x}_r \\ b_\theta &= -\hat{M}_{trim}(\alpha_c) - K_{c,\theta}\hat{I}\tau_{D,\theta}\,\omega_m \\ \mathrm{SP}_x &= \dot{x}_r + \mathrm{clamp}\big(K_x(x_r - x_m), \pm 3\,\mathrm{m/s}\big) \end{aligned} \tag{4.11}$$

with setpoints z_r, SP_x and θ_c against $\mathrm{PV} = z_m$, $v_{x,m}$ and θ_m, and outputs limited to $|a_z| \le 5\,\mathrm{m/s^2}$, $|a_x| \le 3\,\mathrm{m/s^2}$ and $|M| \le 60\,\mathrm{kN\,m}$. Here $\hat{M}_{trim} = \hat{q}S\bar{c}C_m(\alpha_c) - h_p T_p$ is the airframe's moment at the commanded angle of attack and the pusher's, $\hat{q} = \rho\hat{V}^2/2$, and the pitch gain is $K_{c,\theta}\hat{I}$ with $\hat{I}$ the load sheet's inertia. The altitude loop is a PID with $\tau_{I,z} = 12\,\mathrm{s}$, the speed loop a PI with $\tau_{I,v} = 10\,\mathrm{s}$ inside a proportional position trim, and the pitch loop a PD. With $e = \mathrm{SP} - \mathrm{PV}$ and positive gains, an aircraft below, slower than or pitched below its setpoint receives a positive demand in every loop. All three loops are therefore reverse acting, $a = +1$ in the convention of Section 1.3. The pitch loop has no integral action, so its integral term holds only what a manual transfer or a liftoff leaves, multiplied by $\mathrm{e}^{-\Delta t_c/1.5\,\mathrm{s}}$ every step. Manual mode is chosen loop by loop. Individual selections survive before-Run initialization and Reset. The header mode switch sets all three loops together. In manual the operator's demand passes to the allocation and the PID tracks it by choosing I_k, and in the altitude and speed loops the reference follows the aircraft, so the return to automatic is bumpless (Section 1.6.2) and re-plans from where the aircraft is. The references are online jerk-limited profiles of the kind in Section 1.4.4, limited along the route to $1.2\,\mathrm{m/s^2}$ and $0.8\,\mathrm{m/s^3}$ and in height to $0.8\,\mathrm{m/s^2}$, $0.8\,\mathrm{m/s^3}$, 2.5 m/s of climb and 1.5 m/s of descent.

4.5.3 Allocation, Wing First

The allocation works on the estimates. The vertical demand $F_z = \hat{m}(g + a_z)$, less the vertical share of the previous pusher request, is compared with the vertical force the wing makes at the preferred angle, as shown in Equation (4.12).

$$\begin{aligned} \hat{L}_z(\alpha) &= \hat{q}S\left[C_L(\alpha)\cos\hat{\gamma} - C_D(\alpha)\sin\hat{\gamma}\right] \\ \alpha_{pref} &= i_w + (\alpha_{op} - i_w)\,\mathrm{clamp}\big((\hat{V} - 15)/20, 0, 1\big) \\ T_R &= \big[F_z - \hat{L}_z(\alpha_{pref})\big]/\cos\theta_m, \qquad \theta_c = \alpha_c - i_w + \hat{\gamma} \end{aligned} \tag{4.12}$$

with $\alpha_{op} = 9^\circ$ and $\hat{V}$ in m/s. When the wing alone could do more, α_c is lowered to what the demand needs, down to -4°, and the rotors idle at the 570 N collective that holds the more heavily loaded rear group at its 300 N idle thrust. When the rotors cannot supply their share, because of their rating, their spin-up, the timed ramp or the battery, T_R is capped at $T_{R,max}$ and the shortfall is redistributed to the wing by raising α_c, never past $\alpha_s - \Delta\alpha_p = 11^\circ$. What is still missing lights the Z lamp of vertical saturation. Below 12 m/s the wing and the elevator are ignored and the rotors take everything. The pusher then supplies $T_p = (\hat{m}a_x - \hat{F}_{a,x} + T_R\sin\theta_c)/\cos\theta_c$, with $\hat{F}_{a,x}$ the estimated drag force at α_c. A braking demand beyond the pusher's -1.5 kN is redistributed to a nose-up pitch of up to 8° that tilts the rotor thrust aft, never past the protection, and what remains lights the X lamp. If the estimated power exceeds 97 % of the battery's limit, the pusher gives way first and the collective next, which lights the P lamp.

The moment is split by airspeed, as shown in Equation (4.13).

$$\begin{aligned} E_\delta &= \hat{q} S \bar{c} C_{m\delta}, \qquad M_e = w_E M \\ w_E &= \mathrm{clamp}\big((\hat{V} - 20)/20, 0, 1\big) \\ \delta_e &= \mathrm{clamp}(M_e/E_\delta,\ \delta_{min},\ \delta_{max}) \\ \Delta T &= (M - E_\delta \delta_e)/\ell_\Sigma, \qquad \ell_\Sigma = \ell_f + \ell_r \\ T_f &= T_R \ell_r/\ell_\Sigma + \Delta T, \qquad T_r = T_R \ell_f/\ell_\Sigma - \Delta T \end{aligned} \tag{4.13}$$

The elevator's share rises from nothing at 20 m/s to all of the moment at 40 m/s while the rotors turn, and dividing by the estimated effectiveness E_δ schedules its gain with $1/\hat{V}^2$. The collective split in the hover ratio produces no moment, so the differential ΔT carries all of the rotors' share. The differential is served first and limited to the range for which a collective still fits both groups, the collective is then limited to what the differential leaves, and a moment that neither the elevator nor the rotors can make lights the M lamp. A group at its limit therefore costs vertical force, never attitude. This is the moment-first rule of Table 1.1, which Chapter 3 applies to the tilt of a multirotor. The requested commands are rate limited at 25 kN/s for the groups, 10 kN/s for the pusher and 60 °/s for the elevator, and the motors' own current limit, which uses the true airspeed, scales them if their true power would exceed what the battery can give.

4.5.4 The Supervisor

The supervisor flies the mission through the pad, the spool-up, a climb to $h_{tr} = 50$ m, the transition, cruise at $h_{cr} = 110$ m, an approach that begins 3.3 km before pad B, the back-transition, which begins when the along-track reference starts braking, a hover gate over the pad, the vertical descent and the landing. In the feedback transition it stops the rotors only when every condition of Equation (4.14) holds, on measurements and estimates, and the rotors have carried under 8 % of the vertical demand for 2 s.

$$\begin{aligned} &\hat{\mu}_w = \frac{\rho \hat{V}^2 S C_L(\alpha_s - \Delta\alpha_p)}{2\hat{m}g} - 1 \geq \mu_{on}, \qquad \hat{V} \geq 1.2\hat{V}_s \\ &h_m \geq h_{min}, \qquad P_{lim} - P \geq P_{reload}, \qquad \text{airspeeds agree} \end{aligned} \tag{4.14}$$

where $\hat{V}_s$ is Equation (4.8) on the load sheet's mass, $h_{min} = 30$ m, $P_{lim} = P_{max} f(E/E_{cap})$ is the battery's power limit, P the battery's measured power and P_{reload} the power to put the weight back on the rotors at $\hat{V}$. It starts them again after 0.3 s with $\hat{\mu}_w < \mu_{off}$, $\hat{V} < 1.1\hat{V}_s$, $\hat{\alpha}$ within 0.5° of the protection or a disagreement of the airspeeds. On the way down it spins the rotors up once $\hat{V} < V_{spin} = 56$ m/s, or 20 s into the back-transition. The along-track reference does not wait for them, because it is braking into the pad by then and a speed held there could not be braked back within the jerk limit, so V_{spin} alone sets how early they turn. The timed transition caps the collective at $T_{R,max} = 2T_{max}\, r$ with $r = \mathrm{clamp}\big(1 - (t - t_{tr} - t_{u0})/t_u, 0, 1\big)$, where t_{tr} is the start of the transition, $t_{u0} = 28$ s and $t_u = 14$ s, stops the rotors when r reaches zero whatever the airspeed, never restarts them in cruise, and spins them up $t_s = 6$ s after the braking begins.

A vertical landing is feasible when the weaker group can carry its hover share with the margin $\mu_{land} = 10\,\%$, $\min_i(a_i T_{max}/T_{i,trim}) - 1 \geq \mu_{land}$ with a_i the authority left, and the battery can power the hover. The check runs before takeoff, which also needs the charge 3 % above the reserve, and at every step of the flight. In cruise and on the approach a failed check diverts the aircraft on the wing to the airfield, and later a go-around climbs back to h_{tr} on the rotors when that is feasible and fewer than three have been flown, and otherwise diverts if the aircraft is fast enough or above 12 m. The hover gate needs 2 s within 2 m and 0.5 m/s of the pad center within 15 s, and the descent at 1.5 m/s, slowing to 0.5 m/s below 6 m, goes around above 12 m if it drifts 3.5 m off center or its vertical demand stays saturated for 1.5 s. The settings are gathered in Table 4.5.

Three models are kept apart. The simulation model is Section 4.3. The controller's own model is algebraic, made of the same aerodynamic coefficients, the load sheet's mass and inertia, the hover

Table 4.5 Controller, Allocation and Supervisor Settings as Shipped

Symbol	Meaning	Value
$K_{c,z}$, $\tau_{I,z}$, $\tau_{D,z}$	altitude PID	0.3 s^{-2}, 12, 2.2 s
$K_{c,v}$, $\tau_{I,v}$, K_x	speed PI, position trim	0.8 s^{-1}, 10 s, 0.3 s^{-1}
$K_{c,\theta}$, $\tau_{D,\theta}$	pitch PD, times $\hat{I}$	5 s^{-2}, 0.6 s
α_{op}, $\Delta\alpha_p$	preferred angle, protection	9°, 3°
K	vertical-force observer	1.5 s^{-1}
h_{tr}, h_{cr}, V_{cr}	heights, cruise ground speed	50, 110 m, 60 m/s
μ_{on}, μ_{off}	lift margins to stop, restart	35, 15 %
h_{min}, —	stop height, unloaded share	30 m, 8 % for 2 s
V_{spin}	spin-up airspeed	56 m/s
t_{u0}, t_u, t_s	timed schedule	28, 14, 6 s
—	cross-check	15 %, 2 s, above 30 m/s
μ_{land}, —	landing margin, energy reserve	10, 20 %
m_{pay}	payload on the load sheet	250 kg
—	gate window, dwell, longest wait	2 m, 0.5 m/s, 2 s, 15 s

Table 4.6 Scenarios

#	Set-up	Lesson
1	hover 50 m over A, gust at 20 s	the hover split and its cost
2	forward transition from that hover	the load moves, the gate decides
3	wingborne, 42 then 66 m/s at 10 and 70 s	the envelope, hysteresis
4	wingborne 3.2 km out, to pad B	rotors before the wing fades
5	case 2 with a gust at 37 s	measurement against the clock
6	case 2 with 470 kg	gates that move with the load
7	case 2, pitot 12 m/s high at 30 s	an independent airspeed
8	inbound, 470 kg, rear motor fails at 15 s	refusing a landing
9	pad A to B, 470 kg, 40 %, gust at 64 s, timed	graded mission

trim and the power of Equation (4.5), so it errs only through what it cannot measure. The analysis model is Equation (4.8), which interprets the results and enters the code only implicitly, through the gates.

4.6 Measured Cases

Table 4.6 lists the eight cases and the graded mission, which are run as Section 1.6.4 describes. The numbers that follow were produced by the engine run headlessly with the default seed, 20261201, each case as shipped except where a change is stated, and times are simulated seconds from the start of the case. A stated change is made after the case is selected and before Run, and every one quoted here gives the same run when it is carried through a Reset instead. An airspeed at an instant is the true airspeed in force from the control step at that instant, which is how the scorecard records the airspeed of a rotor stop. Table 4.7 gathers the principal outcomes. The exported file carries the true states beside the measured ones, the pitot, lift-derived and trusted airspeeds, the true and estimated angles of attack, the wing and rotor lift beside the weight, the power beside the battery's limit, the phase and rotor state, and the scorecard metrics.

4.6.1 Hover and the Handover

Between 10 and 19.5 s of case 1 the two groups carry the 19.62 kN weight to within 0.02 %, the rear group 10.32 kN and the front 9.30 kN, as the hover trim requires, and the aircraft draws 431 kW, 7.2 kWh a minute. The rotors take 425.7 kW of it, 5.2 kW more than Equation (4.5) gives in still air, because the model charges the rotors for climbing through each updraft of the turbulence and credits nothing on the way down. The pitch loop does not have to hold the unequal split as an error, since the allocation divides the collective in the hover ratio. The gust at 20 s brings the pusher to 300 N of

Table 4.7 Measured Results of Cases 1 to 8

#	Condition	Result
1	hover	$T_R/mg - 1 = 0.02\,\%$, 9.30 and 10.32 kN, 431 kW
1	gust	pusher −300 N, $\lvert\theta\rvert \leq 0.18°$, $x \leq 0.24$ m
2	feedback	492 kW at 2.6 s, half on the wing at 33.5 m/s, gate 48.2 m/s, stop 51.5 m/s at 42.98 s
2	timed	stop 49.8 m/s at 42.00 s
3	60, 42, 66 m/s	4.1°, 139 kW, 9.0° with rotors 13 % and 149 kW, 3.0° and 165 kW
3	speed changes	restart 44.3 m/s at 23.7 s, stop 51.1 m/s at 78.2 s
4	back-transition	spin-up 55.9 m/s, half on the rotors at 32.7 m/s, pitch 5.5°, 464 kW
4	landing	121.6 s, 0.57 m/s, 0.03 m, 8.9 kWh
5	feedback	rotors 9 to 25 %, stop 54.9 m/s at 46.65 s, 1.72 m below
5	timed	stop 39.7 m/s at 42.00 s, 6.7 m below, margin 2.4°
6	feedback	gate 51.0 m/s, stop 53.1 m/s at 44.74 s, timed stop 49.8 m/s
7	cross-check on	lower airspeed 30.73 s, flag 32.72 s, 3.0 m below, stop at 49.3 m/s
7	cross-check off	into the wood at 38.5 s, 856 m along the route
8	470 kg	margin 39.7 to 4.8 %, divert at 15.0 s
8	250 kg	margin 16.3 %, lands at 151.2 s, 0.48 m/s, 0.11 m

reverse thrust, the aircraft moves no more than 0.24 m forward of the pad center, and the pitch stays within 0.18° of level.

Case 2 accelerates from the same hover. Power peaks at 492 kW, 2.6 s in, when the pusher starts while the rotors still carry everything. The rotors carry 97, 86, 42 and 3 % of the weight at 10, 20, 30 and 40 s, at 10.3, 21.7, 34.7 and 47.4 m/s, and the pitch rises to 5.4° as the allocation gives the wing its preferred angle. The altitude stays between 49.3 and 51.9 m through the handover. The estimated rotor share falls under 8 % at 35.55 s, the lift-margin gate opens at 40.95 s, and the rotors stop at 42.98 s at 51.5 m/s, 13.1 m/s above the stall. The timed schedule stops them at 42.00 s at 49.8 m/s, and in this calm air the capacity of 144 % makes the difference invisible.

4.6.2 The Envelope and the Back-Transition

Case 3 starts wingborne at 60 m/s and 110 m. Flown instead at a constant 60, 42 or 66 m/s and averaged from 60 to 150 s, the aircraft draws 139, 149 and 165 kW with the wing at 4.1, 9.0 and 3.0°. At 42 m/s the wing alone would need 10.6°, within 0.4° of the protection, so the allocation keeps it at the preferred 9.0°, and the rotors, restarted, carry 13 % of the weight on 52 kW of which 50 kW is profile power. Slowing from 60 to 42 m/s therefore costs power, 10 kW more, instead of saving it. On the way down the restart comes at 23.7 s at 44.3 m/s, and on the way up the rotors stop again only at 78.2 s at 51.1 m/s. The rotors therefore restart below the 44.6 m/s gate and stop only above the 48.3 m/s one, and between the two they keep whatever state they had, which is the hysteresis of Equation (4.8) and of the safety monitors of Section 1.4.9.

🕮 **Pause.** Try Exercise 4.2 before reading on.

Case 4 starts wingborne at 60 m/s and 50 m, 3.2 km before pad B. Braking starts at 27.6 s, 1.54 km out, and the rotors spin up at 31.5 s at 55.9 m/s, while the wing still carries the whole weight. As the aircraft slows they take what the wing no longer makes and carry half at 51.2 s at 32.7 m/s. With the pusher at its 1.5 kN reverse limit the allocation brakes by pitching up to 5.5°, and the power climbs back to 464 kW by 77.4 s as the aircraft comes to a hover over the pad, where the gate begins at 79.0 s. The 40.5 s descent touches down at 121.6 s at 0.57 m/s, 0.03 m from the center, after 8.9 kWh, and the angle-of-attack margin never falls below 4.1°.

4.6.3 A Gust and a Heavier Load

Case 5 adds a gust from behind at 37 s, 10 m/s along the route and 1 m/s down over 10 s. Before it the rotors carry 9 % of the weight at 42.8 m/s. With the feedback transition the allocation simply gives the rotors back what the wing loses, 25 % of the weight at 42.19 s, the gate stays shut, and the rotors stop at 46.65 s at 54.9 m/s, 3.67 s later than in calm air, with the aircraft never more than 1.72 m below its reference. The timed schedule stops them on the clock at 42.00 s, at 39.7 m/s with a

capacity of 91 %. The vertical demand goes unmet for 3.9 s from 40.9 s, as the ceiling comes down on rotors that the gust is loading again, the aircraft falls 6.7 m below its reference, and the worst angle-of-attack margin shrinks to 2.4°, against 3.8° with the feedback transition.

Pause. Try Exercise 4.1 before reading on.

> **TRY IT IN THE APP 5 · Gust During the Handover**
>
> Load the case and press Run with the Feedback transition. Watch the rotor lift arrows and the Vertical force trend when the gust arrives at 37 s. The rotors take back 25 % of the weight, and they stop only at 46.65 s, at 54.9 m/s, with the aircraft never more than 1.72 m below its reference.

Case 6 carries 470 kg instead of 250 kg, 2220 kg in all. Case 1 flown with that payload hovers on 495 kW, and the estimated stall speed rises from 38.4 to 40.4 m/s. Because the gates are computed from the load sheet, the stop gate opens at 51.0 m/s and the rotors stop at 44.74 s at 53.1 m/s. The timed schedule stops them at 42.00 s at 49.8 m/s, as it would with any payload, and in calm air its capacity of 129 % is still enough. The same schedule meets the gust of case 5 in the challenge.

4.6.4 A Biased Pitot

In case 7 the pitot starts reading 12 m/s high at 30 s, when the true airspeed is 34.7 m/s, so the allocation is told that the wing makes $(46.5/34.7)^2 = 1.8$ times its real lift. With the cross-check on, the lift-derived airspeed disagrees at once. From 30.73 s the allocation trusts the lower of the two, at 32.72 s the pitot is flagged, and from then on the supervisor flies on V_L. The aircraft never falls more than 3.0 m below its reference, and the rotors stop at 41.46 s at a true 49.3 m/s while the pitot reads 61.2 m/s. With the cross-check off, the rotor collective drops from 8.25 to 1.07 kN within half a second of the fault, the aircraft sinks at up to 5.1 m/s, and it comes down on the wood at 38.5 s, 856 m along the route. The Z lamp never lights in that run, because by the allocation's own arithmetic every demand is met.

Pause. Try Exercise 4.3 before reading on.

4.6.5 A Failed Motor

Case 8 flies inbound on the wing with 470 kg. At 15 s one of the four rear motors fails, and the rear group can give 12.0 kN against the 11.45 kN it would carry in a level hover. The lift-group margin falls from 39.7 to 4.8 %, below the 10 % rule, and at 15.00 s the supervisor declares the vertical landing not feasible and diverts to the airfield on the wing, never asking the rear group for thrust it does not have. With 250 kg the rear share is 10.32 kN and the margin 16.3 %, and the aircraft lands on pad B at 151.2 s at 0.48 m/s and 0.11 m from the center, with the rear group working at up to 93 % of what it has left.

4.6.6 The Graded Mission

The challenge lifts off from pad A with 470 kg and the battery at 40 %, begins the transition at 27.11 s and meets the case 5 gust at 64 s, 36.9 s into the transition. It is met with every phase completed, at least 30 s wingborne with the rotors stopped, 25 m of clearance away from the pads, a 2° angle-of-attack margin above 20 m/s, a touchdown slower than 1 m/s no more than 2 m from the pad center, and 20 % of charge or more when it lands, each judged on its worst case. The mission is judged on the case as given, so a changed model parameter or disturbance voids the attempt, and so does an extra disturbance event fired by the learner. The configurations are compared in Table 4.8, and Figure 4.6 draws its distances and stop airspeeds as bars.

As shipped, the timed schedule stops the rotors at 69.11 s, just as the gust has taken the true airspeed down to 37.9 m/s, below the 40.4 m/s stall speed of the loaded aircraft, where even the wing at its lift peak would lift only 88 % of the weight and the protected wing 75 %. The vertical demand had already gone unmet from 67.19 s, as the collective ceiling came down on rotors that the gust

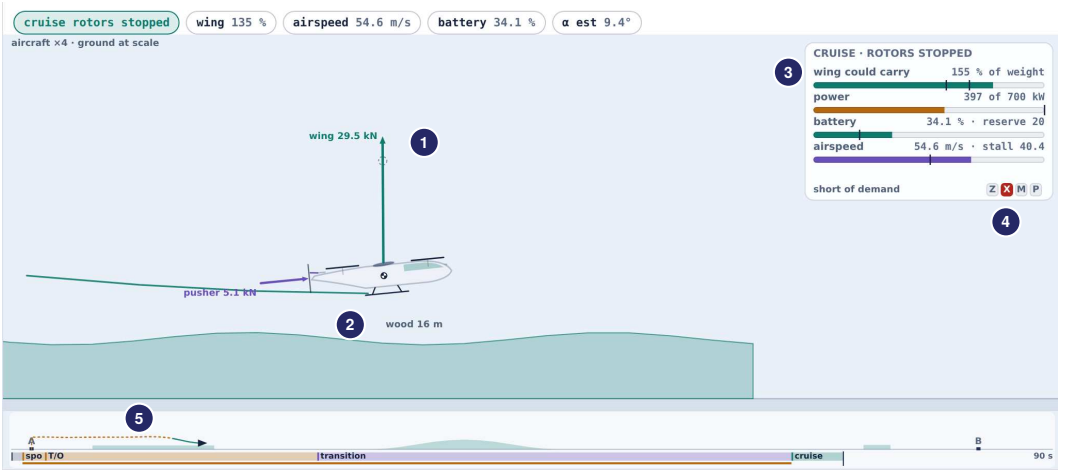


Figure 4.5 The graded mission, Challenge · the full mission, as shipped with the timed transition, paused at $t = 1.23$ min (73.7 s), the lowest point of the flight, 4.6 s after the schedule stopped the rotors, cropped to the plant view. The aircraft (1), drawn four times its size with stopped rotor blades along its booms, is in cruise at 25.4 m, 9.3 m above the wood (2), pitched 5.5° with its wing lifting 29.5 kN, 135 % of the weight, as it pulls out of the sink, and the pusher gives 5.1 kN. The trail in the side view is solid because the rotors were stopped over all of it, and in the route map below it is dotted from pad A to the stop over the wood and solid through the dip (5). The plate reads cruise with the rotors stopped, a wing that could carry 155 % of the weight at the protected angle (3), 397 of 700 kW, 34.1 % of charge and a trusted 54.6 m/s against a 40.4 m/s stall estimate, and the X lamp (4) is lit because the speed loop asks for more than the pusher's 5.5 kN. The trends and the scorecard of the full window are cut.

Table 4.8 Graded Mission at the Default Seed

	Timed	Feedback
rotor stop (s)	69.11	74.42
true airspeed at the stop (m/s)	37.9	55.7
lowest altitude after the gust (m)	25.4	48.1
largest loss below the reference (m)	31.7	1.9
minimum clearance (m)	9.3	32.0
worst angle-of-attack margin (°)	2.2	3.6
longest wingborne interval (s)	80.2	72.8
hover gate over pad B (s)	195.3	195.3
farthest past the pad center (m)	0.21	0.21
touchdown (s)	238.1	238.1
sink (m/s)	0.43	0.43
distance from the center (m)	0.13	0.13
charge at touchdown (%)	25.7	25.6
energy used (kWh)	21.5	21.6
verdict	fail	pass

was loading again. The aircraft sinks at up to 6.2 m/s, from 46.5 m at the stop to 25.4 m at 73.7 s, 9.3 m above the trees, which fails the clearance limit (Table 4.8); Figure 4.5 shows the aircraft at that lowest point. The allocation lowers the nose to keep the angle of attack at its protection as the flight path steepens to −8.4°, and the true angle peaks at 11.8°, so the aircraft sinks rather than stalls. The altitude loop, at its 5 m/s^2 limit and up to 31.7 m behind a reference that climbs toward the cruise



Figure 4.6 The graded mission of Table 4.8 at the default seed, drawn as bars for the timed (solid) and the feedback (hatched) transition. Notice that the timed stop comes below the stall speed of the loaded aircraft, 40.4 m/s (right, dashed line), and that the same flight loses 31.7 m against its reference and passes 9.3 m above the trees, inside the 25 m clearance limit (left, dashed line). The feedback flight keeps 32.0 m of clearance and loses no more than 1.9 m.

altitude, then carries the aircraft back up through that reference to 13.1 m above it at 82.5 s. The overshoot comes from the integral term. Back-calculation with $T_t = \tau_I$ slows it without stopping it, so it grows from 0.09 to 1.33 m/s^2 while the demand is held at the clamp from 69.4 to 76.1 s and peaks at 2.35 m/s^2 at 79.1 s. The rest of the mission is clean, with a 2.2° margin, a touchdown at 0.43 m/s and 0.13 m, and 25.7 % left after 21.5 kWh.

> ⧖ HISTORY **A Conversion Through the Treetops (1979)**
>
> Six days after that first conversion, a test flight called for a maximum acceleration from a low hover over the runway. The nacelles were tilted forward at the maximum rate, at which a conversion from hover to airplane mode can be completed in 12 seconds. The rapid conversion lowered the rotor thrust before the aircraft had the speed for the wing to lift, and the aircraft settled slightly. The crew did not notice the settling until they neared the end of the airfield, and with barely enough speed to climb the aircraft passed through the tops of the trees beyond it. It landed essentially unscathed, with green stains on its blade tips [19]. The timed transition of the graded mission takes the rotor lift away in the same way, before the wing can carry the weight.

The suggested configuration, the feedback transition, keeps the rotors turning through the gust and stops them at 74.42 s at 55.7 m/s. The aircraft never falls more than 1.9 m below its reference, keeps at least 32.0 m of clearance and a 3.6° margin, and flies 72.8 s wingborne. Both flights begin braking into pad B at 143.79 s. The feedback transition spins the rotors up at 147.67 s at 55.9 m/s, and they are up to speed at 53.5 m/s, where the protected wing could still lift 149 % of the weight, while the along-track reference brakes on its jerk-limited profile without waiting for them. The aircraft comes to rest over the pad at most 0.21 m past its center, never drifting back faster than 0.27 m/s, and touches down at 238.1 s at 0.43 m/s, 0.13 m from the center, with 25.6 % left after 21.6 kWh. From 153.2 s on, its position along the route stays within 1 cm of the timed flight's, and the two touchdowns agree to 4 µm. Up to the braking it has used 12.51 kWh against the timed run's 12.49 kWh, and it spends 9.04 kWh from there to the touchdown against 9.01 kWh.

Since the reference never waits, the spin-up airspeed alone decides how much of the wing's margin is left when the rotors take over the weight. Every V_{spin} from 41.5 to 70 m/s, the top of its range, in steps of 0.5 m/s, passes the mission with the same touchdown and a stop within 0.21 m of the pad center, with a worst angle-of-attack margin of 2.2 to 3.6°. The earlier the spin-up, the shorter the wingborne interval, from 84.3 s down to 68.95 s. At 41 m/s the rotors are still spinning up as the

airspeed falls through the 40.4 m/s stall speed of the loaded aircraft, and the margin falls to 1.2°, which fails the mission. Holding the reference's speed while the rotors spin up, as an earlier version of the supervisor did below $1.35\hat{V}_s$, drops its deceleration to zero in the middle of the braking and leaves it to rebuild at the jerk limit. The reference then passes the pad, by 100 m at the default V_{spin} and by 911 m at 52 m/s, and has to fly the aircraft back to it tail first.

Twenty other seeds, 1 to 20, give the same verdicts. The timed schedule stops the rotors at 38.2 to 40.8 m/s and fails 19 of them, 18 on clearance with 10.0 to 24.8 m and 4 on the angle-of-attack margin, and it passes once, with exactly 25.0 m. The feedback transition passes all 20, with 30.4 to 31.9 m of clearance and stops at 55.0 to 57.1 m/s. In every one the aircraft comes to rest over pad B at most 0.43 m past its center and touches down at 0.45 to 0.60 m/s with 25.6 to 25.9 % left.

> ✦ DID YOU KNOW? **Safety Costs Almost No Energy**
>
> From the simulator: in the graded mission the feedback transition flies 72.8 s wingborne against the timed schedule's 80.2 s, and it lands after 21.6 kWh against 21.5 kWh. Only the feedback flight keeps the 25 m clearance, with 32.0 m against 9.3 m (Table 4.8).

4.7 Technology in Practice

The aircraft of Section 4.3 is read by four instruments and moved by two lift-rotor groups, a pusher and an elevator. Figure 4.7 draws the chapter's loops with real devices in their place.

What Measures It

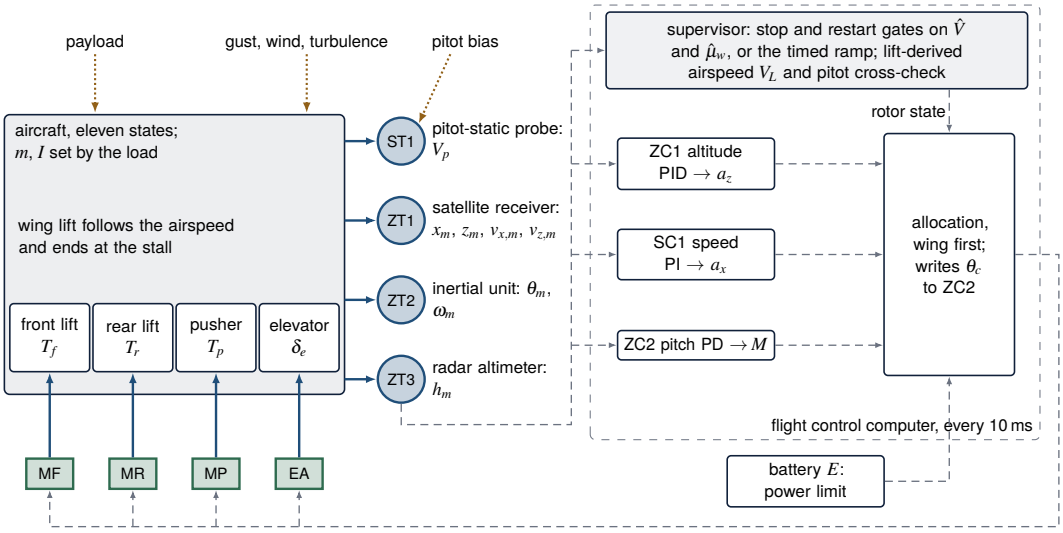
Every gate of Section 4.5 rests on the airspeed, and the airspeed rests on the pitot PT of Figure 4.1. Its 4 Pa of noise and the bias of case 7 stand for the errors of a real probe, and the lift-derived airspeed V_L stands for the independent source a real system compares it with. An unmanned tilt-wing research aircraft listed a pitot-static tube with air data and a combined satellite and inertial unit among its sensors [17], the same set as GN, IMU and PT here.

> TECHNOLOGY **Sensor: Pitot-Static Airspeed**
>
> A pitot tube facing the airflow senses the total pressure, static ports sense the ambient pressure, and the airspeed indicator shows the difference, the dynamic pressure. A wind blowing into the tube makes the same dynamic pressure as motion through still air. Errors almost always mean a blocked tube or port, from moisture, ice, dirt or insects. With the tube blocked and its drain hole open, the indicated airspeed falls to zero, quickly but not at once. With both blocked, it stops following the airspeed and changes with altitude instead [20]. Near hover the output of an airspeed sensor becomes untrustworthy [17], and the chapter's pitot, too, is poor below about 10 m/s.

What Moves It

Each lift group of the model lumps four rotors into one thrust with a lag of 0.15 s, a rate limit of 25 kN/s and a 2 s spin-up, and the supervisor stops and starts the group as a whole. On a real aircraft of this type each lift rotor is driven by its own electric motor, with no mechanical link between the drive systems [3]. A failed motor removes one rotor's thrust, as in case 8, where one of the four rear motors fails.

> TECHNOLOGY **Final Element: Fixed-Pitch Lift Rotors**
>
> Most lift-plus-cruise aircraft proposed have fixed-pitch lift rotors whose thrust is set by their speed [15], with no collective or cyclic pitch. Two-bladed rotors can be indexed to stop aligned with the direction of flight for a small drag penalty, and more than six rotors let controlled flight continue after a failure [3]. With rotor speed control the electric motor sits directly in the control path. A control design to Level 1 handling qualities asked a lift-plus-cruise concept for motor power of 2.15 times its hover power, with heave the most demanding



MF, MR: lift motor drives, lag 0.15 s, spin-up 2 s, up to 16 kN a group. MP: pusher drive, −1.5 to 5.5 kN. EA: elevator actuator, −25 to 20°.

Figure 4.7 The loops of the chapter with real devices in place of the schematic's symbols. ST1 reads the airspeed from a pitot-static probe, ZT1 the position and velocities from a satellite receiver, ZT2 the pitch and its rate from the inertial unit and ZT3 the height from a radar altimeter. One flight control computer (dashed frame) runs the supervisor, the altitude, speed and pitch loops (ZC1, SC1, ZC2) and the allocation every 10 ms. MF and MR are the motor drives of the front and rear lift groups, MP drives the pusher and EA moves the elevator. Notice that the drives of the lift rotors take their commands only from the allocation, and the supervisor reaches them only by setting the rotor state.

axis [15].

Where the Controller Runs

The automatic flight and transition system of the tilt-wing research aircraft ran on a flight control computer in layers: a primary flight control system with stability augmentation, whose gains changed with the wing configuration and the airspeed, an attitude loop above it, guidance loops for altitude, rate of climb, speed and heading, and an auto-transition loop that commanded the configuration [17]. The controller of this chapter has layers of the same kind. Its pitch loop is a PD block, the altitude and speed loops are velocity-form PID blocks (Section 1.6.2), the allocation sits between the loops and the effectors, and the supervisor decides the rotor state. All of them run every 10 ms.

What Is Modernizing It

Three developments bear on the chapter's question of when the rotors may stop. The first is synthetic airspeed. Near hover the research aircraft above replaced its untrustworthy air data with the ground speed below 1.0 m/s [17], and the lift-derived airspeed of this chapter is a cross-check of the same family. The second is unified control, which blends optimal control with a generalized control allocation into a single mode from hover to cruise, without effector sets prescribed for each phase [21]. The third is optimized reference commands for the transition. A cost on the rotor thrusts lets the rotors operate only when necessary and leaves the rest to the wing [22], much as the wing-first rule of Section 4.5 does by construction.

IN PRACTICE **Approach Speed Margins Above the Stall**

Pilots read their stall margins off the airspeed indicator. The low end of its white arc marks the stall speed in the landing configuration, and the low end of the green arc the stall speed in a specified configuration, usually clean at maximum takeoff weight [20]. United States flight training guidance flies the approach at the maker's recommended speed, or at 1.3 times the landing stall speed when there is none, and pilots often add half the gust factor in turbulent air [23]. The gates of this chapter keep the same kind of margin: the stop gate opens at 1.258 times the stall speed, behind an airspeed backstop at 1.2 times.

4.8 Limitations

No real aircraft is modeled, so the numbers say nothing about the performance, energy or safety margins of an actual design. Without roll, yaw or sideslip there are no turns and no crosswind, and each lumped rotor group has neither inflow dynamics, flapping and H-force nor any interaction with the wing. The aerodynamics are quasi-steady, and the stability of the aircraft near the stall is not assessed [16]. The energy reserve is a dispatch rule and a scored limit rather than a reason to divert, so a flight that will land below it is still flown to the pad. The controller's aerodynamic model equals the plant's, and the load sheet is exact, so the gates are as accurate as the airspeed they are given. The pitot cross-check works only above 30 m/s, where the wing carries enough to measure the airspeed by its lift. On the way down the deceleration does not wait for the lift rotors, so a spin-up airspeed set too low leaves the wing near its protected angle until they are up to speed, and at 2220 kg a V_{spin} of 41 m/s or less fails the 2° angle-of-attack margin. The point at which each assumption fails is given in Section 4.3.

OPEN CHALLENGE **Proving a Transition Before It Flies**

In transition the effectors of hover and of wing-borne flight act together. Planning the reference commands and tracking them are both open problems, because redundant effectors leave it unclear how to command each one uniquely [22]. Designs have broken the envelope into phases with a control approach for each, and single control laws from hover to cruise are still examined in simulation [21]. With little flight experience of electric multirotor aircraft, new and rigorous requirements for their response to failures are needed [15]. Progress would be transition laws and failure requirements shown to hold in flight, gusts and heavy loads included.

4.9 Conclusion

A lift-plus-cruise aircraft must earn the stop of its lift rotors, and this chapter put that decision under test on a simulator. Its planar aircraft hovers on 431 kW and cruises on the wing on 139 kW, and closed-form speeds from the weight and the wing place the stop and restart gates within 0.3 m/s of the engine. The lift the wing could make at its protected angle at the moment of the stop predicts the sink, from at most 1.2 m of lost height at 129 to 174 % of the weight to 21.1 m at 75 %. A schedule tuned for 250 kg in calm air stops the rotors at 49.8 m/s there and at 37.9 m/s in the graded mission, below the stall speed of the loaded aircraft, which comes down to 9.3 m above the trees, while the measured gates stop them at 55.7 m/s and keep 32.0 m of clearance. On the way down the aircraft brakes to rest over pad B without waiting for the rotors, which are turning again at 53.5 m/s. A lift-derived airspeed catches a pitot reading 12 m/s high in 0.73 s, and a failed motor that leaves a 4.8 % margin turns the landing into a diversion. The model is planar and quasi-steady, and its controller knows the aerodynamics exactly. A fuller model would add turns and crosswind, rotor and wing interference, dynamic stall, an estimated rather than declared mass and a predictive transition that plans the handover within the envelope. The simulator is a browser plant on which a change of mode granted by a clock and one earned by a measurement can be flown over the same wood and compared.

KEY POINTS

- The lift rotors cost far more power than the wing, so they stop once the wing can carry the weight.
- Closed-form speeds from the weight and the wing place the stop and restart gates within 0.3 m/s of the engine.
- The wing's lift capacity at the stop predicts the sink: at most 1.2 m of lost height at 129 to 174 % of the weight, 21.1 m at 75 %.
- In the graded mission a schedule tuned in calm air stops the rotors at 37.9 m/s, below the stall speed of the loaded aircraft, while the measured gates stop them at 55.7 m/s.

Where else this applies. Volume 8, Chapter 11 also ends a step on a measurement rather than on the clock, and Volume 4, Chapter 12 shares one demand among effectors with hard limits.

References

[1] T. A. Johansen and T. I. Fossen, "Control allocation—a survey," *Automatica*, vol. 49, no. 5, pp. 1087–1103, 2013.

[2] D. Liberzon and A. S. Morse, "Basic problems in stability and design of switched systems," *IEEE Control Systems*, vol. 19, no. 5, pp. 59–70, 1999.

[3] C. Silva, W. R. Johnson, E. Solis, M. D. Patterson, and K. R. Antcliff, "VTOL urban air mobility concept vehicles for technology development," in *2018 Aviation Technology, Integration, and Operations Conference*. American Institute of Aeronautics and Astronautics, 2018.

[4] A. Kasliwal, N. J. Furbush, J. H. Gawron, J. R. McBride, T. J. Wallington, R. D. De Kleine, H. C. Kim, and G. A. Keoleian, "Role of flying cars in sustainable mobility," *Nature Communications*, vol. 10, no. 1, p. 1555, 2019.

[5] A. Keller, F. Gandhi, R. Niemiec, and A. Walter, "Full flight regime controller design for a Lift+Cruise eVTOL aircraft," *Journal of the American Helicopter Society*, vol. 71, no. 3, pp. 1–22, 2026.

[6] B. W. Bequette, "Process control practice and education: Past, present and future," *Computers & Chemical Engineering*, vol. 128, pp. 538–556, 2019.

[7] J. A. Rossiter, B. Pasik-Duncan, S. Dormido, L. Vlacic, B. Jones, and R. Murray, "A survey of good practice in control education," *European Journal of Engineering Education*, vol. 43, no. 6, pp. 801–823, 2018.

[8] D. H. Jacobson, "An evaluation of lift engines in tactical VTOL aircraft," *Journal of Aircraft*, vol. 2, no. 5, pp. 424–429, 1965.

[9] V. Jackson and D. Patch, "Design and development of the primary fly-by-wire flight control system for the XV-4B V/STOL research aircraft," in *Control and Flight Dynamics Conference*. American Institute of Aeronautics and Astronautics, 1968.

[10] J. Magee and K. Wernicke, "XV-15 tilt rotor research aircraft - program report," in *Atlantic Aeronautical Conference*. American Institute of Aeronautics and Astronautics, 1979.

[11] H. Glauert, "The theory of the autogyro," *The Journal of the Royal Aeronautical Society*, vol. 31, no. 198, pp. 483–508, 1927.

[12] R. W. Beard and T. W. McLain, *Small Unmanned Aircraft: Theory and Practice*. Princeton: Princeton University Press, 2012.

[13] W. C. Durham, "Constrained control allocation," *Journal of Guidance, Control, and Dynamics*, vol. 16, no. 4, pp. 717–725, 1993.

[14] J. M. Buffington and D. F. Enns, "Lyapunov stability analysis of daisy chain control allocation," *Journal of Guidance, Control, and Dynamics*, vol. 19, no. 6, pp. 1226–1230, 1996.

[15] W. Johnson and C. Silva, "NASA concept vehicles and the engineering of advanced air mobility aircraft," *The Aeronautical Journal*, vol. 126, no. 1295, pp. 59–91, 2022.

[16] J. P. Spadão, R. M. G. Vasconcellos, M. Sartorato, and W. M. dos Santos, "Dynamic stability and control authority blending in lift-plus-cruise eVTOL transition flight," *Dynamics*, vol. 6, no. 2, p. 21, 2026.

[17] K. Muraoka, T. Yokoyama, N. Yokoyama, and M. Sato, "Flight verification of automatic flight and transition system for lift/cruise thrust type VTOL aircraft," *Transactions of the Japan Society for Aeronautical and Space Sciences*, vol. 67, no. 5, pp. 285–294, 2024.

[18] F. Larocque, T. De Ponti, B. Remes, and E. Smeur, "Synthetic air data system for pitot tube failure detection on the variable skew quad plane," in *AIAA SCITECH 2025 Forum*. American Institute of Aeronautics and Astronautics, 2025.

[19] M. D. Maisel, D. J. Giulianetti, and D. C. Dugan, *The History of the XV-15 Tilt Rotor Research Aircraft: From Concept to Flight*, ser. Monographs in Aerospace History. Washington, DC: National Aeronautics and Space Administration, NASA History Division, 2000, no. 17, nASA SP-2000-4517, https://ntrs.nasa.gov/citations/20000027499.

[20] Federal Aviation Administration, "Pilot's handbook of aeronautical knowledge," FAA-H-8083-25B, Chapter 8, Flight Instruments, https://www.faa.gov/sites/faa.gov/files/regulations_policies/handbooks_manuals/aviation/phak/10_phak_ch8.pdf, 2016.

[21] M. J. Acheson, I. M. Gregory, and J. Cook, "Examination of unified control incorporating generalized control allocation," in *AIAA Scitech 2021 Forum*. American Institute of Aeronautics and Astronautics, 2021.

[22] J. L. Bullock, S. Cheng, A. Patterson, M. J. Acheson, N. Hovakimyan, and I. M. Gregory, "Reference command optimization for the transition flight mode of a lift plus cruise vehicle," in *AIAA SCITECH 2024 Forum*. American Institute of Aeronautics and Astronautics, 2024.

[23] Federal Aviation Administration, "Airplane flying handbook," FAA-H-8083-3C, Chapter 9, Approaches and Landings, https://www.faa.gov/sites/faa.gov/files/regulations_policies/handbooks_manuals/aviation/airplane_handbook/10_afh_ch9.pdf, 2021.

4.10 Exercises

4.1 ○ Concept check · 2 min

In scenario 5 a gust from behind arrives at 37 s, during the handover. With the timed transition the rotors stop at 42.00 s. At that instant the ground speed is 49.6 m/s, close to the 49.7 m/s of scenario 2 in calm air at the same instant, but the true airspeed is 39.8 m/s. Why has the wing lost lift?

(a) The gust slows the aircraft over the ground, and the lift follows the ground speed

(b) The downdraft of the gust tilts the lift backward without changing its size

(c) The pitot reads low in the gust, so the allocation lowers the angle of attack

(d) Lift follows the velocity relative to the air, and wind from behind subtracts from it

4.2 ○ Concept check · 1 min

In scenario 3 the cruise speed is cut to 42 m/s and later raised to 66 m/s. The supervisor restarts the rotors at 44.3 m/s on the way down and stops them only at 51.1 m/s on the way up. What is the gap between the restart margin $\mu_{off} = 15\,\%$ and the stop margin $\mu_{on} = 35\,\%$ for?

(a) It keeps turbulence near one airspeed from starting and stopping the rotors again and again

(b) It gives the rotors their 2 s of spin-up before the wing runs short of lift

(c) It corrects for the pitot, which reads differently while slowing and while accelerating

(d) It keeps the rotors stopped for as long as possible to save their profile power

4.3 ○ Concept check · 2 min

In scenario 7 with the airspeed cross-check off, the pitot starts reading 12 m/s high at 30 s. The aircraft sinks into the wood at 38.5 s, yet the Z lamp of vertical saturation never lights. Why?

(a) The lamp is switched off together with the cross-check, so no fault can be shown

(b) The allocation sizes the wing's share with the biased airspeed, so by its own arithmetic every demand is met

(c) The altitude error stays too small for the loop to ask for more lift than the wing makes

(d) The bias stops the rotors, so neither group can reach a limit that would light the lamp

4.4 ▭ Theory and calculation · 7 min

Each lift group sits $\ell = 2.9\,\mathrm{m}$ from the rotors' centroid, and the center of mass lies 0.15 m behind the centroid ($c = -0.15\,\mathrm{m}$). The aircraft has a mass of 2000 kg with $g = 9.81\,\mathrm{m/s^2}$. Each group has a disk area $A = 20\,\mathrm{m^2}$, a figure of merit $FM = 0.75$ and a profile power $P_0 = 25\,\mathrm{kW}$, and $\rho = 1.225\,\mathrm{kg/m^3}$.

(a) Find the thrust of each group in a level hover in still air, and the share of the weight the rear group carries. *Checkpoint:* $T_f = 9.30\,\text{kN}$, $T_r = 10.32\,\text{kN}$, 52.6 %.

(b) Find the power the two groups draw in that hover from Equation (4.5). *Checkpoint:* 420.5 kW.

(c) Find the ideal induced power $\sum T_i v_h$ and the effective figure of merit, the ideal power divided by the power of part (b). *Checkpoint:* 277.9 kW and 0.661.

4.5 Theory and calculation · 7 min

Use $C_{L,max} = 1.359$ at the lift peak, $C_L = 1.159$ at the protected angle of 11°, $S = 16\,\text{m}^2$, $\rho = 1.225\,\text{kg/m}^3$ and $g = 9.81\,\text{m/s}^2$. The aircraft carries 470 kg of payload, 2220 kg in all.

(a) Find the stall speed V_s and the protected speed V_p of Equation (4.8). *Checkpoint:* 40.4 m/s and 43.8 m/s.

(b) Find the stop gate V_{on} and the restart gate V_{off} for $\mu_{on} = 35\,\%$ and $\mu_{off} = 15\,\%$. *Checkpoint:* 50.9 m/s and 47.0 m/s.

(c) The timed schedule of the graded mission stops the rotors at a true airspeed of 37.9 m/s. Find the share of the weight the wing can lift at that speed at the protected angle and at the lift peak. *Checkpoint:* 75 % and 88 %.

4.6 Theory and calculation · 5 min

A lift group is rated at 16 kN with four motors. With 2220 kg on board, one of the four rear motors fails, so the rear group can give three quarters of its rating. Use the hover shares of the arms $\ell_f = 3.05\,\text{m}$ and $\ell_r = 2.75\,\text{m}$, $g = 9.81\,\text{m/s}^2$, and the landing rule $\min_i(a_i T_{max}/T_{i,trim}) - 1 \geq 10\,\%$.

(a) Find the margin of the weaker group after the failure. *Checkpoint:* 4.8 %, the rear group.

(b) Find the largest total mass that still meets the rule, and the largest payload on the 10 kg grid of the Payload control for an empty mass of 1750 kg. *Checkpoint:* 2114.7 kg, so 360 kg.

4.7 App challenge · 8 min

Load scenario 5, Gust during the handover, with the default seed, and run at speed 5. Use the scorecard tiles Rotors stopped at, Peak altitude loss and Worst angle-of-attack margin.

(a) Run as shipped, with the Feedback transition, to 60 s, and read the three tiles. *Checkpoint:* 54.9 m/s, 1.7 m and 3.8°.

(b) Press Reset, set Transition to Timed before Run, run to 60 s and read the same tiles. *Checkpoint:* 39.7 m/s, 6.7 m and 2.4°.

(c) In the exported file of the second run, read `speed_mps` and `airspeed_mps` at 42.00 s, within 0.2 m/s. Then find the share of the weight the wing can lift at the protected angle at the stop airspeed, with $V_p = 41.6\,\text{m/s}$ at 2000 kg. *Checkpoint:* 49.6 m/s and 39.8 m/s, a capacity of 91 %.

4.8 App challenge · 8 min

Load scenario 7, Airspeed bias, with the default seed, and run at speed 5.

(a) Run as shipped, with the cross-check On, until the Transition logic card reports ROTORS STOPPED. Read the Rotors stopped at and Peak altitude loss tiles, and find in the exported file the first row in which `airspeed_disagree` is 1. *Checkpoint:* 49.3 m/s with the pitot at 61.2, 3.0 m, and the row at 32.75 s.

(b) Press Reset, set Airspeed cross-check to Off before Run, and run until the run stops by itself. Read the Mission tile, and find in the file the first row in which `phase` reads `crashed`, with its time and `x_m` within 1 m. *Checkpoint:* Crashed, at 38.55 s and 856 m.

(c) In the same file, read `rotor_lift_z_kN` at 30.00 and 30.50 s, and explain the change. *Checkpoint:* 8.23 and 1.07 kN.

4.9 App challenge · 8 min

Load the challenge, the full mission, with the default seed, and run at speed 10. Each flight lasts about 240 s and pauses itself after the landing.

(a) Fly it as shipped, with the Timed transition. Read the Min clearance, Rotors stopped at, Peak altitude loss and Worst angle-of-attack margin tiles, and say which part of the target fails. *Checkpoint:* 9.3 m, 37.9 m/s, 31.7 m and 2.2°. The clearance fails.

(b) Press Reset, set Transition to Feedback before Run, and fly the whole mission. Read Min clearance, Worst angle-of-attack margin, Wingborne, rotors stopped, Touchdown and Battery at the end. *Checkpoint:* 32.0 m, 3.6°, 73 s longest, 0.43 m/s at 0.13 m, 25.6 %.

4.10 Application area · 4 min

The engine measures 431 kW in hover at 2000 kg, 139 kW in wingborne cruise at 60 m/s, and 149 kW at 42 m/s, where the restarted rotors carry 13 % of the weight on 52 kW, of which 50 kW is profile power.

(a) Find the energy of one minute of hover and of one minute of cruise at 60 m/s, and the energy per kilometer of cruise at 60 and at 42 m/s. *Checkpoint:* 7.2 and 2.3 kWh, then 0.64 and 0.99 kWh per kilometer.

(b) A dispatcher proposes flying the approach at 42 m/s to save energy, because the airframe drag falls with the square of the speed. Say why the power rises instead. *Checkpoint:* The wing needs more angle than the allocation allows, so the rotors restart and their profile power outweighs the drag saved.

4.11 Application area · 4 min

The chapter's controller knows the payload exactly from the load sheet, and its pitot cross-check works only above 30 m/s.

(a) Suppose the load sheet says 250 kg while 470 kg is on board. The stop gate is computed from the sheet. Where does it open, and what share of the true weight can the wing lift there at the protected angle? Use the speeds of Equation (4.8) at 2000 and 2220 kg. *Checkpoint:* At 48.3 m/s, 122 % instead of the intended 135 %.

(b) Why can the cross-check not work at low airspeed, and what does a practicing engineer have to add for that part of the flight? *Checkpoint:* The wing makes too little lift to infer an airspeed from it.

4.12 Review the agent · 6 min

An AI assistant reports: "Raising the altitude loop's Integral time from 12 to 60 s cures the challenge. The sink over the wood was integral windup in the altitude loop, so the shipped Timed transition is safe and the measured gates are not needed." The challenge fires its gust 36.9 s after the transition starts. Test the claim with the default seed at speed 10, then find the flaw. Each flight pauses itself after the landing, near 256 s.

(a) Load the challenge, set Integral time to 60 s before Run, keep the Timed transition and fly the mission. Read the Min clearance, Rotors stopped at and Worst angle-of-attack margin tiles. *Checkpoint:* 19.4 m, 38.9 m/s and 2.6°. The clearance fails.

(b) Press Reset, keep Integral time at 60 s, set Transition to Feedback before Run and fly it again. Read Min clearance and the verdict. *Checkpoint:* 31.3 m, and every part passes.